Glassiness through the emergence of effective dynamical constraints in interacting systems



2002 J. Phys.: Condens. Matter 14 1571

(http://iopscience.iop.org/0953-8984/14/7/314)

INSTITUTE OF PHYSICS PUBLISHING JOURNAL OF PHYSICS: CONDENSED MATTER

J. Phys.: Condens. Matter **14** (2002) 1571–1579 PII: S0953-8984(02)31606-0

# Glassiness through the emergence of effective dynamical constraints in interacting systems

**Juan P Garrahan**

Department of Physics, Theoretical Physics, University of Oxford, 1 Keble Road, Oxford OX1 3NP, UK

E-mail: j.garrahan@physics.ox.ac.uk

Received 5 December 2001
Published 7 February 2002
Online at stacks.iop.org/JPhysCM/14/1571

**Abstract**

I describe a class of spin models with short-range plaquette interactions, whose static equilibrium properties are trivial, but which display glassy dynamics at low temperatures. These models have a dual description in terms of free defects subject to effective kinetic constraints, and are thus an explicit realization of the constrained dynamics picture of glassy systems.

## 1. Introduction

Perhaps the simplest systems which display the slow cooperative relaxation characteristic of glasses are the facilitated kinetic Ising models, first introduced in [1], in which glassiness is not a consequence of either disorder or frustration in the interactions, but of the presence of kinetic constraints in the dynamics of the system. Depending on the nature of the constraints these models may behave as strong [1–3] or fragile [4,5] glasses, display stretched-exponential relaxation [6, 7], fragile-to-strong transitions [7], etc.

Kinetically constrained systems are interesting for several reasons. First, they are usually free of disorder or frustration, and the interactions imposed by the constraints are short ranged. Second, their equilibrium static properties are trivial, so their glassiness is a purely dynamical effect, in contrast to the case for mean-field models [8] where statics and dynamics are closely related [9]. Third, their low-temperature behaviour is dominated by activated processes, which, although highly relevant for supercooled liquids near the glass transition, are not taken into account by mode-coupling theory [10] or in mean-field theory [11]. Finally, the simplicity of these models may allow for exact solutions or at least a thorough analytical description of their behaviour, which can help one to understand dynamically arrested systems in general.

The rationale behind the kinetically constrained approach was most clearly given in [6]: it should be possible to describe the dynamics of a strongly interacting system which displays glassy behaviour in terms of hierarchies of degrees of freedom, from fast to slow, independent of the presence of disorder or even frustration; these hierarchies would be weakly interacting in the energetic sense, but their dynamics should be constrained, the faster modes constraining

  

the slower ones. Systems with explicit kinetic constraints, like the spin-facilitated models or the constrained lattice gases [12, 13], represent one side of this picture, but concrete examples in which this full scenario is realized are much harder to find. The purpose of this paper is to address this issue by describing a simple class of models of interacting spins with 'normal' dynamics which have a dual description in terms of free excitations whose dynamics is subject to effective kinetic constraints. They are thus an explicit realization of the constrained dynamics scenario of [6].

## 2. Models

Consider the following model: a system of Ising spins $\sigma = \pm 1$ on a triangular lattice, where each spin interacts in triplets with its nearest neighbours lying at the vertices of a downward-pointing triangle [15, 16]:

$$H_3 = -J \sum_{ijk \in \nabla} \sigma_i \sigma_j \sigma_k. \tag{1}$$

This system belongs to a class of models of Ising spins interacting with their neighbours through plaquette interactions, such that the spins and bonds reside in isomorphic lattices and there is one bond per spin. The simplest example is the one-dimensional Ising model (see e.g. [14]). In two dimensions, in addition to model (1), there is the plaquette model on the square lattice [17]:

$$H_4 = -J \sum_{ijkl \in \square} \sigma_i \sigma_j \sigma_k \sigma_l \tag{2}$$

which is a special case of Baxter's eight-vertex model [14]. These models can be generalized to higher dimensions. Four spins interacting in the corners of downward-pointing tetrahedra of an fcc lattice would be a generalization of (1), while eight-spin interactions in the vertices of cubes of a simple cubic lattice would generalize (2). The sign of the couplings is irrelevant for large systems, and even disordered $\pm J$ can be absorbed by a rescaling of the spins. In what follows $J > 0$ is assumed.

Below I will mainly focus on the triangular model of equation (1), but it will be instructive to compare with the 1D Ising model and the square plaquette model (2).

## 3. Spin–defect duality

The common feature of the class of models of the previous section is that they all have, for appropriate boundary conditions, a one-to-one mapping between spin and bond (or 'defect') configurations. For the Ising model on the line, this happens if one boundary is fixed, say, $\sigma_0 = 1$, and the other free. In this case the spin-to-bond mapping and its inverse simply read

$$b_i \equiv \sigma_{i-1}\sigma_i \Rightarrow \sigma_i = \prod_{j=1}^{i} b_j. \tag{3}$$

Similarly, for the square plaquette model there is a one-to-one mapping if the spins on one boundary row and column are fixed, say, $\sigma_{i0} = \sigma_{0i} = 1$, and the other boundary is left free:

$$b_{ij} \equiv \sigma_{i-1\,j-1}\sigma_{ij-1}\sigma_{i-1\,j}\sigma_{ij} \Rightarrow \sigma_i = \prod_{k,l=1}^{i,j} b_{kl}. \tag{4}$$

Notice that, while the bonds are defined locally in terms of their surrounding spins, the inverse mapping is non-local. In order to derive it I made implicit use of the effect of introducing an

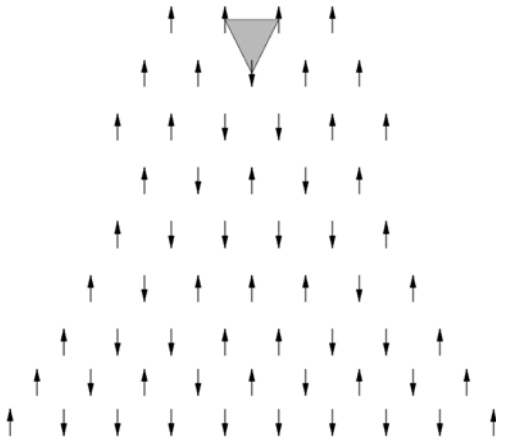

**Figure 1.** The PT of down spins formed by the presence of a defect, shown as a shaded triangle, in the triangular plaquette model.

excitation in the ground-state configuration $\sigma = 1$, i.e., of how the spin configuration has to be rearranged to avoid any further defects.

For the more interesting case of the triangular plaquette model the situation is more complicated. The spin-to-bond mapping is again straightforward:

$$b_{ij} \equiv \sigma_{ij}\sigma_{ij+1}\sigma_{i-1j+1} \tag{5}$$

where the indices $i$ and $j$ run along the unit vectors of the triangular lattice $\vec{a}_1 \equiv \hat{x}$ and $\vec{a}_2 \equiv \frac{1}{2}(\hat{x} + \sqrt{3}\hat{y})$. The inverse map can be obtained from the following observation [18]. A ground state of the system can be constructed row by row: the state of one row of spins determines the following one. A row configuration can be specified by a dipolynomial (i.e., a generalization of a polynomial containing terms with both positive and negative powers of the argument) $P(z) = \sum_n (1 - 2\sigma_n)z^n$, where $\sigma_n$ are the spins on the row, and $n$ runs from $-L/2$ to $L/2$, where $L$ is the horizontal length of the system. The following row $\sigma'$ is then given by $P'(z) = \hat{T}P(z)$, where $\hat{T} = 1 + z$ is the operator which propagates rows, and the coefficients in $P'$ are taken modulo 2. Suppose a defect is created at position $n = 0$ in a ground state of all spins up. The row just below the defect has a spin down at $n = 0$ and its dipolynomial is $P(z) = 1$. Then the $m$th row below it will be given by $P^{(m)}(z) = \hat{T}^m = (1 + z)^m \bmod 2$, which means that the propagation of the original spin down produces other down spins at the positions for which the combinatorial numbers $\binom{n}{m} \bmod 2$ are non-zero, a structure known as a Pascal triangle (PT); see figure 1. The spin configuration due to a configuration of defects is obtained by the superposition mod 2 of the PTs that each individual defect generates and the ground state on which the excitation has been produced.

If the system is of linear length a power of two and has periodic boundary conditions in at least one direction, then there is a unique ground state given by all spins up, and the spin–bond mapping is one-to-one [15]. Moreover, the dipolynomial $P(z)$ has to be taken modulo $1 + z^L$ (spins $\sigma_1$ and $\sigma_{L+1}$ are identified), and, since $\hat{T}^L \bmod 2 = 1 + z^L$, the propagation described above stops at the $L$th row. For this case equation (5) can be inverted: the spin at site $ij$ is given by the superposition of the PTs of all the defects $b_{kl} = -1$ with $i - l \leqslant k \leqslant i$ and $l \geqslant j$:

$$\sigma_{ij} = \prod_{l=j}^{j+L-1} \prod_{k=i-l}^{i} b_{kl}^{\binom{l-j}{i-k}}. \tag{6}$$

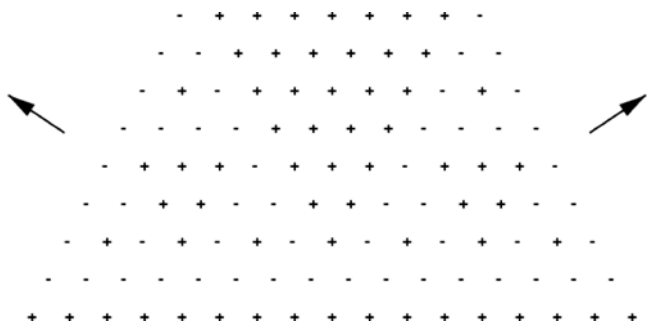

**Figure 2.** An example of a symmetry transformation of $H_3$. Spins denoted by '$-$' are inverted.

Equation (6) is analogous to equations (3) and (4). An important difference is that, while for the 1D Ising and square plaquette models a spin in the bulk is the product of $\mathrm{O}(L^d)$ defects, for the triangular model it is given the product of $\mathrm{O}(L^{d_f})$ defects, where $d_f = \ln 3/\ln 2$ is the fractal dimension of the PT. Similar considerations apply to the higher-dimensional models.

## 4. Symmetries

Consider now the symmetries of $H_3$. Suppose a whole row of spins is inverted. None of the bonds below that row is affected since pairs of spins on the row interact with spins in the next one. To leave the bonds immediately above unchanged it is necessary to invert every other spin in the preceding row. As one goes up, the situation becomes more complicated, but eventually it can be seen that if one inverts two PTs of spins, as shown in figure 2, $H_3$ remains invariant. The choice of the initial row of flipped spins and the column from which the PTs stem is arbitrary, as is the orientation of the transformation, which can be in the three symmetry directions of the problem. This gives a total of $3N$ transformations. However, a bit of algebra with binomial coefficients shows that there are at most $2L$ independent symmetry operations. First, by combining transformations in two of the symmetry directions, say $\vec{a}_1$ and $-\vec{a}_2$, one gets a transformation in the third direction, $\vec{a}_2 - \vec{a}_1$. Second, only the choice of row is free, since the central column can be shifted by superposition of transformations in different rows.

The number of symmetries has to be the same as the number of ground-state configurations. By looking at the cycles of the operator $\hat{T}$ [18], it can be shown that in general there are at most $\mathrm{O}(L)$ ground states. For the special case of periodic boundary conditions of length a power of two, for which the ground state is unique, it is not difficult to prove that any transformation like that of figure 2 'wraps' around on itself and becomes trivial. In that case $H_3$ has no exact symmetries.

Once again, the symmetries of $H_3$ are a complicated analogue of the ones in the 1D Ising model, which simply has the global inversion symmetry, and the square plaquette model, where $H_4$ is left invariant by the inversion of any row or column. In both these cases they are exact symmetries only for periodic or free boundary conditions.

## 5. Statics

With the information of the two previous sections it becomes easy to calculate the static properties of the models. If for each case the boundary conditions are chosen such that the spin–defect mapping is one to one, the bonds are non-interacting and the partition function is

simply that of a system of $N$ free Ising excitations, $Z_N = 2^N \cosh^N(J/T)$. Now, for both the 1D Ising model and the square plaquette model, we know from exact diagonalization of their transfer matrices [14] that for arbitrary boundary conditions the partition function per site in the thermodynamic limit is

$$\kappa \equiv \lim_{N\to\infty} Z_N^{1/N} = 2\cosh(J/T). \tag{7}$$

In the case of the triangular model, for linear size $L = 2^K$ with periodic boundary conditions, the row-to-row transfer matrix has a single non-zero eigenvalue equal to $\kappa^L$. For arbitrary boundary conditions it can be checked by numerical diagonalization that the largest eigenvalue is still $\kappa^L$, so in the thermodynamic limit the partition function per site is given by (7) irrespective of the boundaries. Probably this can be proved using the exact methods of [14]. Similar evidence suggests that for the higher-dimensional models equation (7) holds too.

The expectation value of bonds is

$$\langle b\rangle = \tanh(J/T) \tag{8}$$

and the equilibrium energy density is, up to constants, just the concentration $c$ of defects

$$c = \tfrac{1}{2}[1 - \tanh(J/T)]. \tag{9}$$

Using equations (3)–(5) all spin correlation functions can be calculated. Since in all models a spin in the bulk is the product of $O(N^\delta)$ bonds (the precise power depending on the model), in the limit of $N \to \infty$, one obtains

$$m \equiv \langle\sigma\rangle = 0 \tag{10}$$

for all $T > 0$, i.e., all models are disordered at any finite temperature.

Arbitrary correlation functions are computed in a similar manner:

$$\langle\sigma_i \cdots \sigma_j\rangle = [\tanh(J/T)]^{\mathcal{N}_{i\cdots j}} \tag{11}$$

where $\mathcal{N}_{i\cdots j}$ is the number of bonds which enter in the definition of the product of spins $\sigma_i \cdots \sigma_j$. Only operators for which $\mathcal{N}_{i\cdots j}$ is finite in the thermodynamic limit have non-vanishing expectation values. As usual, the 1D Ising model is the simplest; the product of two spins $\sigma_i\sigma_j$ corresponds to the product of all the bonds in between, giving the usual exponential decay of correlations with separation. In the square plaquette model all two- and three-point spin correlations vanish. The first non-trivial correlations are for quartets of spins in the vertices of rectangles, which correspond to the product of all enclosed bonds.

In the case of the triangular plaquette model the simplest non-vanishing correlations are for triplets of spins located at the vertices of downward-pointing equilateral triangles of side length $2^k$, which are given by the product of all the enclosed defects which also belong to the corresponding PT:

$$C^{(3)}_{2^k} = \langle\sigma_{ij}\sigma_{ij+2^k}\sigma_{i-2^k,\,j+2^k}\rangle = [\tanh(J/T)]^{3^k}. \tag{12}$$

Notice the exact scaling relation $C^{(3)}_l = [C^{(3)}_1]^{l^{\,d_f}}$.

The fact that most of the correlation functions are zero is a consequence of the multiple symmetries of these models and there being no symmetry breaking in the thermodynamics: only spin products which are invariant under *all* the symmetry operations can have non-zero correlations.

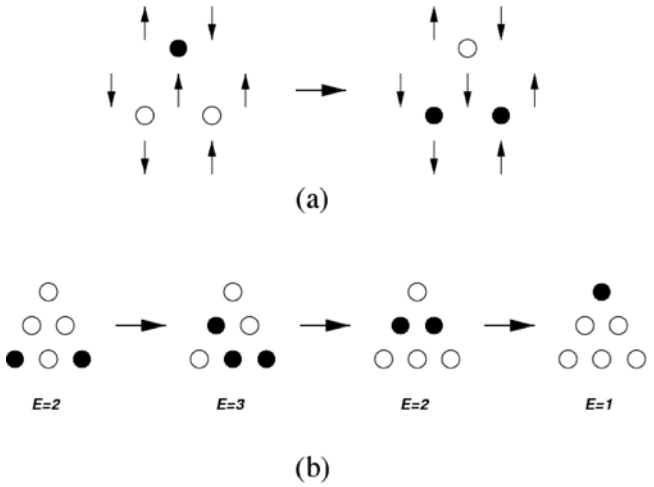


**Figure 3.** (a) An example of a spin-flip move. Defects are represented as dark circles. (b) Activated relaxation of a pair of defects at a distance $l = 2$.

## 6. Dynamics

While the statics of the class of models being discussed here is trivial, their dynamics is not. Under a single-spin-flip dynamics like Glauber or Metropolis all of these models, except, of course, the 1D Ising, become dynamically arrested due to the appearance of energy barriers for the relaxation.

Consider the case of the triangular model. A single spin flip corresponds to flipping the three bond variables around it; see figure 3(a). This means that an isolated defect is locally stable since any change in the spins around it creates a new pair of defects and thus increases the energy. Moreover, only pairs of defects at a distance $l = 2^k$ can be relaxed by means of local spin moves, and the energy barrier is $\Delta E = k$ (where we have set $J = 1/2$); see figure 3(b). As the system relaxes it has to cross barriers which grow as the logarithm of the size of equilibrating regions.

From the observation that barriers grow logarithmically it is straightforward to estimate the equilibration time. The rate of relaxation of an excitation of linear size $l$ is given by the Arrhenius formula $\Gamma(l) \sim \exp(-\ln l/T \ln 2)$. Thus, after time $t$ the average linear distance between defects is $l \sim t^{T \ln 2}$. The equilibrium value of this distance at low $T$ is $l_{\mathrm{eq}} = c^{-1/2} \sim \exp(1/2T)$, and hence the equilibration time is

$$\tau \sim \exp\left(\frac{1}{2T^2 \ln 2}\right). \tag{13}$$

This supra-Arrhenius form is known as the Bässler equation [19] and corresponds to fragile behaviour in the classification of Angell [20]. The absence of any finite-temperature singularity is consistent with the fact that the model has no finite-temperature phase transition.

The existence of a hierarchy of energy barriers implies that the dynamics takes places in stages corresponding to the relaxation of a typical length scale at each stage. This is clearly seen in the decay of the concentration of defects after a quench from $T = \infty$ to a low temperature; see figure 4(a). After an initial $T$-independent exponential relaxation corresponding to the (barrierless) removal of pairs of neighbouring defects, the concentration displays 'plateaus', which are the more pronounced the lower the temperature. These plateaus are the result of

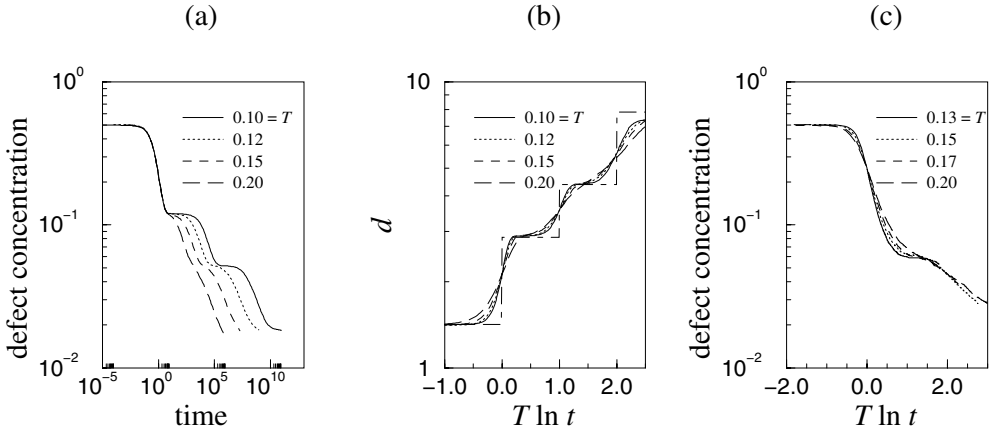


**Figure 4.** (a) Concentration of defects as a function of time following a quench from $T = \infty$ to various $T$, from MC simulations of model (1). (b) Average distance between defects as a function of rescaled time $T \ln t$. The dot–dashed curve corresponds to the analytic approximation. (c) Decay of the concentration of defects as a function of rescaled time, in the three-dimensional model of four spins interacting in the corners of downward-pointing tetrahedra of an fcc lattice.

the system becoming trapped in locally stable configurations, and correspond to the different stages of the dynamics.

The dynamical behaviour of the triangular plaquette model is almost identical to that of the asymmetrically constrained Ising chain (or East model) [4, 5]. In fact, the typical distance between defects (as well as the complete distribution of distances) at each stage of the dynamics can be computed approximately using the independent-interval method of [5]. Figure 4(b) shows that the agreement between theory and simulations is reasonably good [16]. This means that in terms of the defect variables, the dynamics is effectively constrained as in the East model. The existence of a dual description in terms of interacting spins with standard dynamics on the one hand, and in terms of free defects subject to effective kinetic constraints on the other, makes this model an explicit realization of the constrained dynamics scenario [6].

The dynamics of the square plaquette model is somewhat simpler, although still activated. Since a pair of neighbouring defects can diffuse freely, isolated excitations only face barriers of constant size. Its glassy dynamics is strong, like that of the Fredrickson–Andersen model [1,3]. The dynamics of the defects is effectively given by the constrained lattice models of covalent networks of [21].

The generalization to three dimensions of the triangular model is that of spins on an fcc lattice interacting with four-spin interactions between nearest neighbours on the corners of downward-pointing tetrahedra. The energy barrier to the relaxation of excitations at a distance $2^k$ is in this case $2k$. In this model there are zero-energy moves when two defects are next to each other, but, in contrast to the case for the square model, these are not diffusive since every pair belongs only to one plaquette. The relaxation time is of the Bässler form, $\tau \sim \exp[2/(3T^2 \ln 2)]$, and the behaviour is again fragile. Figure 4(c) shows the decay of the concentration of defects after a quench to low temperatures. Notice that the length of the plateaus is now two units of rescaled time $T \ln t$.

The symmetry considerations of the previous sections also apply to the dynamics. Since the evolution operator has the same symmetries as the Hamiltonian, dynamical expectation values of non-symmetric operators will vanish if the initial configuration is taken from a

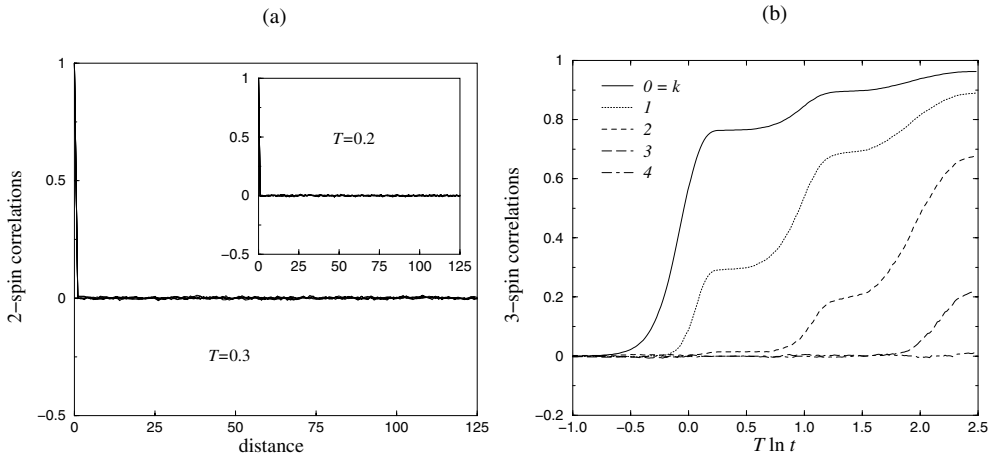


**Figure 5.** (a) Two-spin correlations in the triangular model for times $t = 1$, 10, $10^2$, $10^3$, $10^4$, and $10^5$ as a function of distance. (b) Three-spin correlation functions $C_k^{(3)}$ as a function of time, for linear sizes $2^{k=0,1,2,3,4}$, at $T = 0.12$.

distribution which is also invariant, irrespective of whether the system is in equilibrium or not, as in the out-of-equilibrium regime after a quench from an initial infinite-temperature state. This can be illustrated with the triangular model. Figures 5(a) and (b) show that all two-point spin correlation functions vanish at all times after the quench, while the invariant combination of triplets of spins in downward triangles of length a power of two has a non-trivial behaviour over time. Figure 5(b) also shows how the stages of the dynamics correspond to the relaxation of regions of size $2^k$.

## 7. Conclusions

I have discussed a class of non-disordered and non-frustrated spin models with local plaquette interactions which display glassy behaviour due to the presence of energy barriers to the relaxation. The low-temperature dynamics is effectively that of free excitations subject to dynamical constraints.

While rather unrealistic, these models have several interesting features. They are explicit realizations of both sides of the constrained dynamics scenario. Since the dynamics is defined through their Hamiltonian, glassiness is not a consequence of *ad hoc* dynamical rules, as in models with imposed kinetic constraints. The fact that their statics is trivial but their dynamics glassy is consistent with recent observations in more realistic models [22]. And all the interesting behaviour happens in the activated regime.

## Acknowledgments

I warmly acknowledge the collaboration of Mark Newman in much of the work described here. I would also like to thank David Chandler and Arnaud Buhot for important discussions. This work was supported by the Glasstone Fund (Oxford).

## References


[1] Fredrickson G H and Andersen H C 1984 *Phys. Rev. Lett.* **53** 1244
[2] Schulz M and Trimper S 1999 *J. Stat. Phys.* **94** 173
[3] Crisanti A, Ritort F, Rocco A and Sellitto M 2001 *J. Chem. Phys.* **113** 10 615
[4] Jäckle J and Eisinger S 1991 *Z. Phys.* B **84** 115
[5] Sollich P and Evans M R 1999 *Phys. Rev. Lett.* **83** 3238
[6] Palmer R G, Stein D L, Abrahams E and Anderson P W 1984 *Phys. Rev. Lett.* **53** 958
[7] Buhot A and Garrahan J P 2001 *Phys. Rev.* E **64** 21 505
[8] Kirkpatrick T R and Thirumalai D 1987 *Phys. Rev. Lett.* **58** 2091
[9] Franz S, Mézard M, Parisi G and Peliti L 1998 *Phys. Rev. Lett.* **81** 1758
[10] Götze W and Sjögren L 1992 *Rep. Prog. Phys.* **55** 55
[11] Bouchaud J P, Cugliandolo L F, Kurchan J and Mézard M 1997 *Spin-Glasses and Random Fields* ed A P Young (Singapore: World Scientific)
[12] Kob W and Andersen H C 1993 *Phys. Rev.* E **48** 4364
[13] Kurchan J, Peliti L and Sellitto M 1997 *Europhys. Lett.* **39** 365
[14] Baxter R J 1982 *Exactly Solved Models in Statistical Mechanics* (London: Academic)
[15] Newman M E J and Moore C 1999 *Phys. Rev.* E **60** 5068
[16] Garrahan J P and Newman M E J 2000 *Phys. Rev.* E **62** 7670
[17] Lipowski A 1997 *J. Phys. A: Math. Gen.* **30** 7365
[18] Martin O, Odlyzko A M and Wolfram S 1984 *Commun. Math. Phys.* **93** 219
[19] Bässler H 1987 *Phys. Rev. Lett.* **58** 767
[20] Angell C A 1995 *Science* **267** 1924
[21] Davison L, Sherrington D, Garrahan J P and Buhot A 2001 *J. Phys. A: Math. Gen.* **34** 5147
[22] Santen L and Krauth W 2000 *Nature* **405** 550